9. Buttiker M, Landauer R *J. Phys. C Solid State Phys.* **21** 6207 (1988)
10. Steinberg A M, Kwiat P G, Chiao R Y *Phys. Rev. Lett.* **71** 708 (1993)
11. Nimtz G, Enders A, Spieker H *J. Physique I* **4** 565 (1994)
12. Milonni P W *J. Phys. B At. Mol. Opt. Phys.* **35** R31 (2002)
13. Shvartsburg A B et al. *Phys. Rev. E* **78** 016601 (2008)
14. Einstein A "On the electrodynamics of moving bodies", in *The Collected Papers of Albert Einstein* Vol. 2 *The Swiss Years: Writings, 1900–1909* (Eds J Stachel et al.) (Princeton, N.J.: Princeton Univ. Press, 1989)

PACS numbers: **43.20.+g**, **43.30.+m**, **43.60.–c**
DOI: 10.3367/UFNe.0181.201111k.1217

Focusing of low-frequency sound fields on the ocean shelf

V G Petnikov, A A Stromkov

1. Introduction

The utility of focused low-frequency (100–500 Hz) sound for solving a variety of applied tasks of sea-shelf acoustics is presently a subject of ongoing research. The case in point concerns focusing of sound waves at distances of several dozen kilometers from focusing systems in a sea with a typical depth of 100 m.

From a physical viewpoint, the question to be answered is how to focus sound waves in a planar waveguide, the parameters of which (depth, refractive index, and acoustic characteristics of the lower boundary set by the oceanic bottom) are some complex functions of space coordinates. It is essential that part of these parameters, primarily the refractive index, exhibit random fluctuations in space and time. Furthermore, the distance to the focal point far exceeds the size of the focusing system.

Under these circumstances, perhaps the only way to focus sound waves consists in adopting methods based on the generation by the focusing system of a wave field that is conjugate to the medium. Such methods include the wave front reversal (WFR) (or phase conjugation) of sound waves and a similar approach based on time wave reversal [1–3], dubbed the time-reversal mirror (TRM). It should be kept in mind that both methods rely on detecting sound waves emitted by a probe source (PS) placed at the supposed focal point and subsequent generation of the reversed wave field by the focusing system backwards into the waveguide. Sound propagation in the opposite direction through just the same inhomogeneities as encountered on the direct way leads to the compensation of phase and time distortions of the acoustic signals and, as a result, to focusing on the PS site.

This paper describes methods and research results related to unusual properties of focused sound in shallow water. It discusses characteristics of physical setups designed for focusing sound waves in conditions that are very experimentally demanding. It also considers possible areas where the focused sound can be utilized.

V G Petnikov A M Prokhorov General Physics Institute, Russian Academy of Sciences, Moscow, Russian Federation
E-mail: petniko@kapella.gpi.ru
Stromkov A A Institute of Applied Physics, RAS, Nizhny Novgorod, Russian Federation

Uspekhi Fizicheskikh Nauk **181** (11) 1217–1222 (2011)
DOI: 10.3367/UFNr.0181.201111k.1217
Translated by S D Danilov; edited by A Radzig

2. Methods of the investigation of focused sound in shallow water

Studies of specific features of sound focusing in ocean shelf have been carried out both through numerical simulations and on-site experiments (see, for example, Refs [4–6]). Generally, the TRM-based focusing effect in some vicinity of point $\mathbf{r}_0$ was computed for the spatial distribution of the quantity $B(\mathbf{r})$:

$$B(\mathbf{r}) = \max_t \big(B_c(\mathbf{r}, t)\big) = \max_t \left[\frac{1}{T}\left|\int_{-\infty}^{\infty} P(\omega, \mathbf{r})\, s(\omega) \exp(-i\omega t)\,d\omega\right|\right]. \quad (1)$$

The function $B_c(\mathbf{r}, t)$ represents here the envelope of the cross-correlation function of the transmitted and received retransmitted signals, which can, strictly speaking, be defined for broadband signals of finite duration; the maximum is sought with respect to time t; $\mathbf{r}_0$ is the radius vector of the focal point (the point where the PS is located); $s(\omega)$ is the spectrum of the transmitted signal; T is its duration, and $P(\omega, \mathbf{r})$ is the spectrum of the retransmitted signal at some point $\mathbf{r}$:

$$P(\omega, \mathbf{r}) = \sum_j^J Z_1(\omega, \mathbf{r}_j, \mathbf{r})\, Z^*(\omega, \mathbf{r}_0, \mathbf{r}_j)\, s^*(\omega)\,, \quad (2)$$

with the asterisk $*$ denoting a complex conjugation. Here, $Z(\omega, \mathbf{r}_0, \mathbf{r}_j)$ and $Z_1(\omega, \mathbf{r}_j, \mathbf{r})$ are the waveguide transfer functions between points $\mathbf{r}_0$ and $\mathbf{r}_j$, and $\mathbf{r}_j$ and $\mathbf{r}$, respectively, and, finally, $\mathbf{r}_j$ is the radius vector of transceivers (receiving and emitting elements) of the focusing system. It is assumed that the role of such a system is played by a discrete vertical antenna composed of J transceivers (just such antennae are used in conventional hydroacoustic on-site experiments to transmit and receive low-frequency hydroacoustic signals).

When applied to the focusing of a quasiharmonic sound field of frequency $\omega = \omega_0$ and arbitrarily long duration, formula (1) converts to the well-known expression for the field amplitude at the observation point:

$$P_a(\omega_0, \mathbf{r}) = \left|\sum_j^J Z_1(\omega_0, \mathbf{r}_j, \mathbf{r})\, Z^*(\omega_0, \mathbf{r}_0, \mathbf{r}_j)\right| s_0\,. \quad (3)$$

Formula (3) describes focusing with the help of WFR for a harmonic PS with the amplitude s_0. As shown by Zverev [3], the two methods of focusing (based on WFR and TRM) possess principal distinctions, which has just been corroborated by numerical modeling.

In numerical simulations, the transfer functions were taken as sums of interacting waveguide modes. In particular, the following expression served to compute the $Z(\omega, \mathbf{r}_0, \mathbf{r}_j)$ function:

$$Z(\omega, \mathbf{r}_0, \mathbf{r}_j) = \sum_m^{M(\omega)} C_m(\omega, \mathbf{r}_0, \mathbf{r}_j)\, \frac{\psi_m(\omega, z_j)}{\sqrt{q_m(\omega) r_0}} \exp\big(i q_m(\omega) r_0\big)\,, \quad (4)$$

where $\psi_m(\omega, z)$ and $\xi_m(\omega)$ are the eigenfunctions (waveguide modes) and eigenvalues of the related Sturm–Liouville problem $[\xi_m(\omega) = q_m(\omega) + i\gamma_m(\omega)/2]$, respectively, and $M(\omega)$ is the number of propagating modes. The expression for $Z_1(\omega, \mathbf{r}_j, \mathbf{r})$ is written out in a similar way [6].

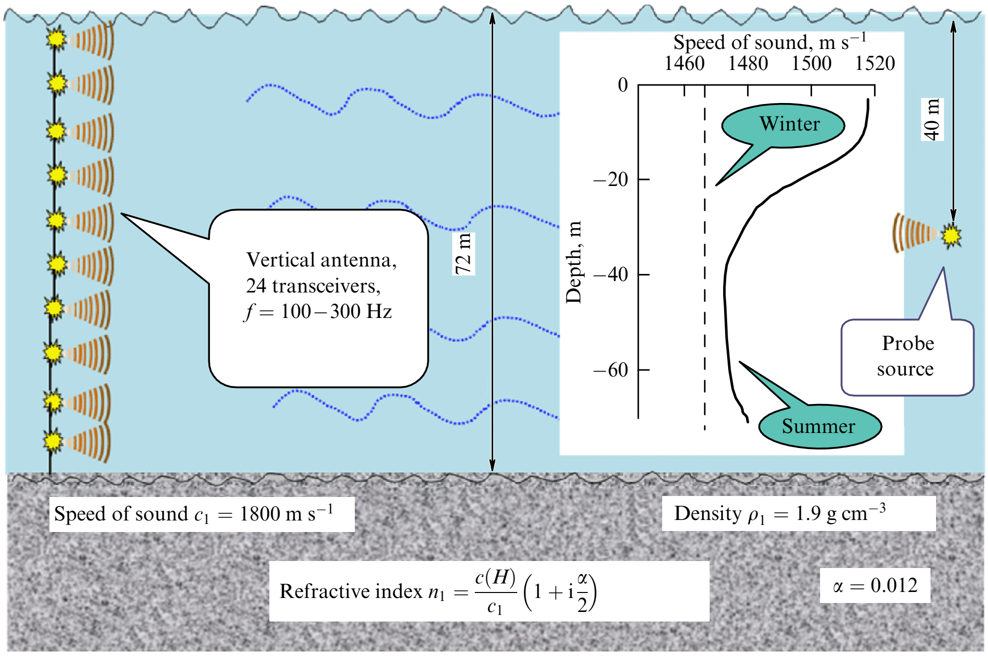

Figure 1. Schematics and parameters of numerical modeling.

The coefficients $C_m(\omega, \mathbf{r}_0, \mathbf{r}_j)$ are found by solving the system of differential equations for interacting modes in the range of distances from the probe source to the receiving–transmitting element of the antenna [6]. The key aspect of these equations is the coefficient of intermodal interaction, which depends on the form of space–time perturbations of the refractive index (the speed of sound) in the waveguide. On the sea shelf, these perturbations are primarily brought about by surface waves and, during the summer season, also by internal-gravity waves.

Modeling of a sound field focusing involves the solution of a more general problem on the interaction of waves of different natures on the oceanic shelf. The solution method was proposed in Ref. [7]. We only mention here that this method exploits the spatio–temporal power spectra of random vertical fluid displacements in the field of gravity and surface waves. For the field of background internal waves in the shelf zone, such spectra (noticeably varying among ocean sites) are measured in experiments including radar observations of surface manifestations of internal waves. For the surface waves, one may apply the known empirical relationships for the wind waves spectrum (for example, the Neyman–Pearson relationship).

Thus, by using relationships (1) and (3), it appears possible to compute the focused sound field in the vicinity of the probe source with a TRM and a WFR. Of primary interest is the field calculation in the vertical plane passing through the focusing antenna and the PS. In a cylindrical reference frame centered at the antenna, this is the (r, z, φ_0) plane, where r is the distance, z is the depth, and φ_0 is the angle specifying direction to the source. The noteworthy feature of this problem — also the one of practical significance — is the fact that in a horizontally homogeneous waveguide in the absence of random perturbations (for example, under calm weather conditions in winter), focusing occurs in any vertical (r, z, φ) plane, and not only in the PS plane, provided, certainly, that the waveguide parameters are independent of φ. Put differently, the focal region in this case looks like a torus. Admittedly, this case in not a typical one. More probable is the situation where a weak dependence of the waveguide parameters on the angle φ still exists, and the focal region takes the form of a toroidal segment.

Given modern computational capabilities, the calculation of a focused sound field in the (r, z, φ_0) plane with the required spatial resolution does not face practical difficulties. Figure 1 shows the schematics and parameters of a numerical experiment on sound focusing in a typical ocean shelf region, the results of which are described in Section 3. Their salient features, mentioned below, were tested and observed by us in numerical simulations spanning a sufficiently broad range of parameters (not only those of Fig. 1) characteristic of the focusing problem in a shallow water.

In contrast, measurements of spatial characteristics of a sound field in the (r, z, φ_0) plane are hardly possible under natural conditions. This would require the deployment of a large number of vertical receiver arrays in this plane. Under the assumption that the PS shares its location with one of the receivers in these arrays ($r_0 = r_{q'}$, $z_0 = z_{n'}$), formulas (1) and (3) can be rewritten as

$$B(r_q, z_n) = \max_t \left[\frac{1}{T} \left| \int_{-\infty}^{\infty} \sum_j^J Z_1(\omega, z_j, r_q, z_n) \times Z^*(\omega, r_{q'}, z_{n'}, z_j) \left| s(\omega) \right|^2 \exp(-\mathrm{i}\omega t)\, \mathrm{d}\omega \right| \right], \quad (5)$$

$$P_{\mathrm{a}}(\omega_0, r_q, z_n) = \left| \sum_j^J Z_1(\omega_0, z_j, r_q, z_n)\, Z^*(\omega_0, r_{q'}, z_{n'}, z_j) \right| s_0 \,. \quad (6)$$

The spatial resolution and size of the tested domain will be determined by the number of arrays and the distance between the receivers.

At present, the results of on-site experiments with only one array are available [4], which has enabled one to

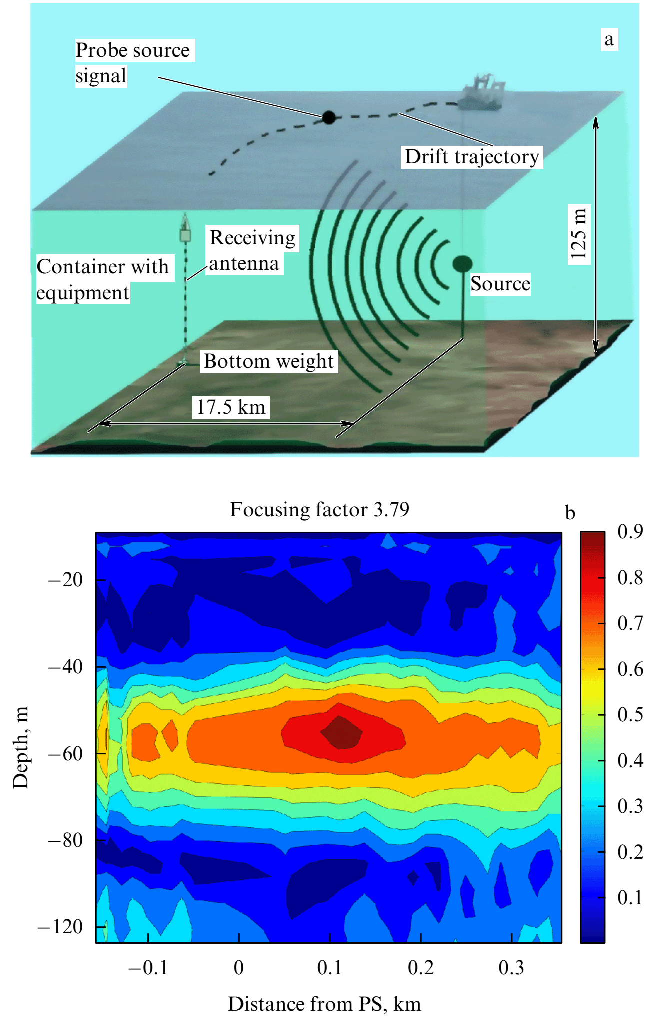

Figure 2. (a) Schematics and parameters of the on-site experiment in the Barents Sea. (b) Focusing of sound field in the frequency range 100–300 Hz.

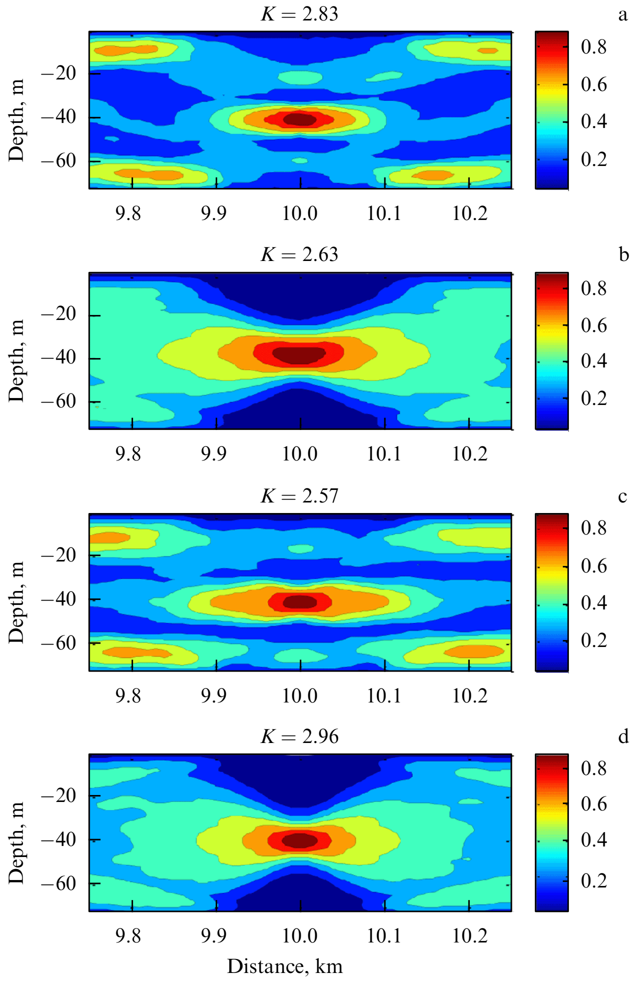

Figure 3. Focusing of the sound field by using TRM (numerical simulations): a single transceiver at a depth of (a) 9 m, (b) 40 m, and (c) 63 m; (d) focusing vertical antenna.

measure the vertical distribution of sound pressure in the focal spot and its evolution with time. This experiment, however, was carried out in a closed sea-shelf region characterized by gentle stratification and weak surface waves, i.e., in the absence of random perturbations in the sound speed profile. Under these circumstances, i.e., in the approximation of a 'frozen' medium, there exists a simpler technique of assessing the quality of focusing, implemented in our experiments [5]. We mean a combined method of estimating the quality of focusing, which incorporates measurements of waveguide transfer functions and subsequent computation of the focused sound field. Naturally, the reversibility of the transfer function with respect to exchanging the source and sound receiver is assumed to be granted.

The measurement technique is schematically illustrated in Fig. 2 which depicts a research vessel towing a source of sound toward the receiving antenna. The towing track, which passes through the supposed sound focal point, is located in the (r, z, φ_0) plane. Recording the known signal from the sound source enables the transfer functions $Z(\omega, r_0, z_0, \varphi_0, z_j)$ and $Z_1(\omega, z_j, r_q, z_{n'}, \varphi_0)$ to be measured and then, using Eqns (5) and (6), the sound field distribution over the focal spot to be computed.

3. Specific features of sound focusing on sea shelves

Specific features of low-frequency sound focusing in shallow water stem from the waveguide character of sound field propagation. First and foremost among them, we should mention the possibility of focusing with the help of a single transceiver if the TRM is applied and a broadband acoustic field is induced.[1]

Figure 3 demonstrates an example of such focusing (hereinafter we consider the distribution $B(r, z)$ normalized on its maximum value) at a distance of ≈ 10 km. In modeling it was assumed that the probe source emits a signal with a linear frequency modulation in the band $f = 100-300$ Hz. As a rough estimate of focusing quality, Fig. 3 also shows the computed value of the coefficient $K = \max\,(B(r,z))/\langle B(r,z)\rangle$ commonly referred to as the focusing factor.[2] Here, $\max\,(B(r,z))$ implies the maximum value of the quantity $B(r, z)$ varying over the ranges of r and z specified in Fig. 3, and $\langle B(r,z)\rangle$ is the mean value over those intervals excluding the focal point.

[1] Thus, focusing in a waveguide is analogous to that with the help of a single transceiver in a strongly scattering medium [2].

[2] Notice that for focusing quasiharmonic sound fields with the help of the WFR, we can similarly write out the expression for K which will feature $P_a(r, z)$ instead of $B(r, z)$.

As can be seen from Fig. 3, the quality of focusing provided by the vertical antenna is only slightly better than that offered by a single transceiver. The quantity K, however, does not reflect certain aspects of focusing procedure. For example, the character of focusing for a single transceiver depends on the depth. If the transceiver is placed at the same depth z_0 as the PS, the sound field is concentrated in the region of the focal spot, although the spot size is somewhat larger than with the vertical antenna. If the transceiver is located in some proximity to the waveguide boundaries, the size of the focal spot is approximately the same as for the vertical antenna. However, in such cases the field distribution is characterized by side maxima, which are absent when the transceiver is located at z_0 or if the antenna is used. These peculiarities are caused by the dependence of the excited mode spectrum on the depth of the sound source immersion.

The feasibility of focusing with the help of a single transceiver was also confirmed by computations that utilized transfer functions measured in a real experiment (see Fig. 2). The bandwidth of transmitted acoustic signals was $f = 100$–300 Hz. Computations of the focused field were performed by a formula for a single transceiver located at the depth z_j [5]:

$$B(r_q, z_n) = \max_t \left[\frac{1}{T} \left| \int_{-\infty}^{\infty} Z(\omega, r_q, z_{n'}, z_n) \times Z^*(\omega, r_{q'}, z_{n'}, z_j) \left| s(\omega) \right|^2 \exp(-\mathrm{i}\omega t)\, \mathrm{d}\omega \right| \right], \tag{7}$$

where $n = 1, 2, \ldots, J$. Formula (7) coincides with the exact expression (5) only for points lying at the trajectory of sound source motion in the on-site experiment. Nevertheless, numerical results indicated that this formula correctly describes sound focusing in the (r, z, φ_0) plane.

We also emphasize that the quality of focusing for a single transceiver and the TRM essentially depends on the relative bandwidth $\Delta f/f$ of the sound field. Numerical simulations indicated that, under typical conditions of shallow water, the magnitude of $\Delta f/f$, which keeps the focusing factor above 2.5, exceeds 40%.

When employing WFR, focusing of the sound field with the help of a single transceiver becomes impossible. In this case, one needs to apply extended vertical antennae spanning the entire depth of the shallow water waveguide. Figure 4 demonstrates the results of focusing with a WFR at different frequencies for harmonic acoustic signals [computations rely on Eqn (6)]. As could be anticipated, the quality of focusing rises when the frequency increases. The comparison of Figs 3 and 4 gives evidence that the quality of focusing with the TRM and WFR is largely similar provided that the WFR of acoustic waves with frequency $f = 200$ Hz is used, i.e., the frequency which is equal to the mean frequency of linear-frequency-modulated (LFM) signals utilized for the TRM.[3] It turned out simultaneously that the quality only weakly depends on the number of transceivers for the same total length of focusing antenna (Fig. 4b, d). Conversely, the quality of focusing sharply drops if the length of the antenna is reduced but the number of transceivers is preserved. The fact that the separation between transceivers becomes decreasingly smaller compared to $\lambda/2$ (λ being the wavelength of sound) does not lead to a substantial impact. In particular, the results of computations indicate the absence of any focusing if the antenna length $L \leqslant 0.2H$ (H is the waveguide depth) and if the depth of immersion of the antenna phase center noticeably differs from that of the probe source. Noteworthy, all these effects derive from the waveguide's sound propagation.

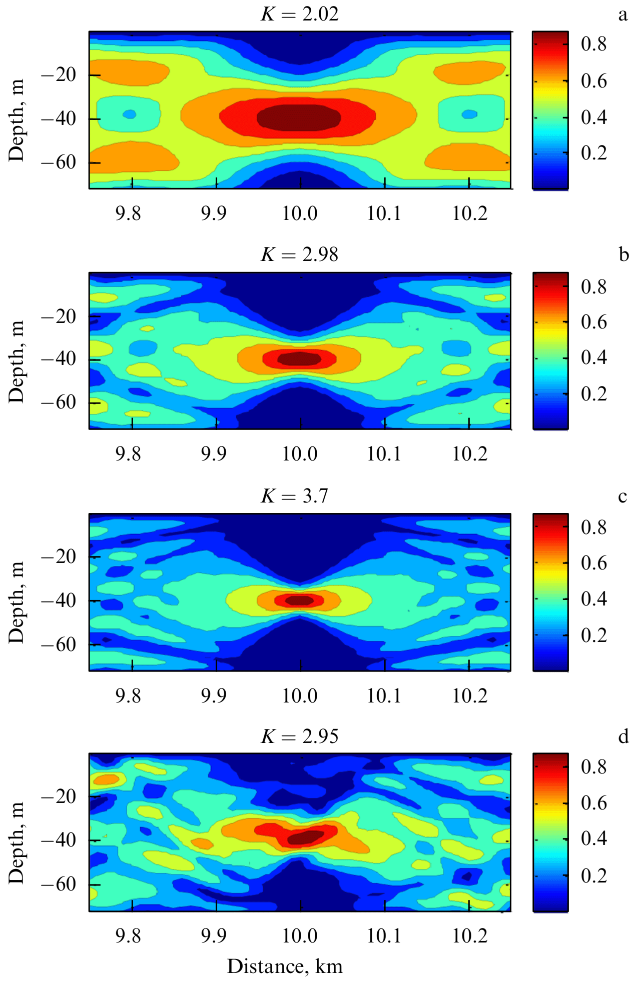

Figure 4. Focusing of the sound field by using WFR (numerical simulations): (a) $f = 100$ Hz, 24 transceivers; (b) $f = 200$ Hz, 24 transceivers; (c) $f = 300$ Hz, 24 transceivers, and (d) $f = 200$ Hz, 5 transceivers.

The size of the focal spot in the (r, z, φ_0) plane depends on the distance r to the focusing system, this dependence, however, being weak compared to the similar dependence for the domain of vertical wave field localization in the free space, as provided by a linear vertical antenna ($D_\perp \approx r\lambda/L$). The size of the focal spot also depends on the number M of energy-carrying waveguide modes at the site of the probe sound source. Because of sound damping, the effective number M of modes reduces with the distance, and the size of the focal spot increases. For the waveguide sketched in Fig. 1, Table 1 lists the sizes of focal spots (on the level of 0.7)

Table 1

Spot size, m / Distance r, km	$D_\perp$	$D_\parallel$
10	10.3	104
30	18.8	410

[3] Here, we compare the quality of focusing achieved with one and the same antenna.

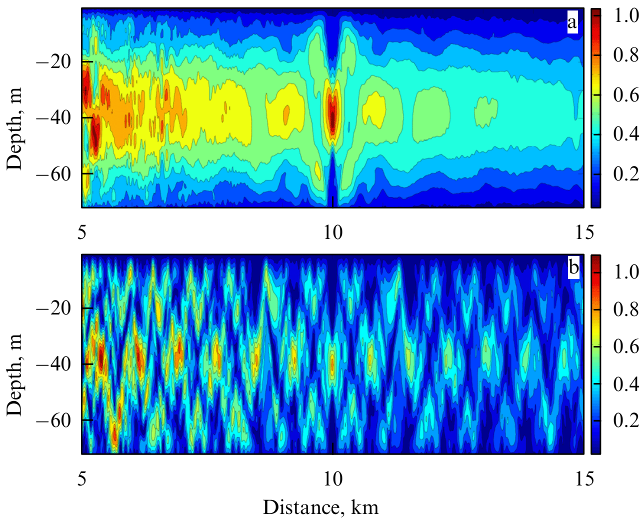

Figure 5. The interference structure of focused acoustic radiation in a shallow-water waveguide. The PS resides at the distance of 10 km, and depth of 40 m. (a) TRM with a single transceiver at the point $r = 0$ and $z_j = 40$ m. (b) WFR with the focusing antenna spanning the total depth at the origin of the coordinates.

computed with the help of formula (6). Here, $D_{\perp}$ and $D_{\parallel}$ are the vertical and horizontal focal spot sizes, respectively. The sound radiation frequency is $f = 200$ Hz.

The focused field behaves in a specific way not only in the vicinity of PS. In fact, focusing reshapes the interference patterns of the sound field throughout the waveguide. The emerging interference structure (it is referred to as the speckle structure in optics) is characterized by the formation of secondary focal spots located both before and behind the PS with respect to the focusing system. Examples of such a structure are furnished by Fig. 5 for both the TRM and WFR cases. As is apparent from the figure, the appearance effect of secondary focal spots is manifested more strongly for the WFR.

In the interval spanning several hundred meters in the horizontal plane, the position of the focal spot can be changed without resorting to repeated focusing with the help of the PS. One only needs to change the radiation frequency of the focusing antenna by several hertz, preserving the amplitude–phase distribution across its aperture. Notice that not only the position of the main focal spot, but also the positions of the secondary spots mentioned above change in this case. Thus, we get a possibility of scanning by focused sound waves.

As time progresses, spatio–temporal perturbations on the sea shelf substantially deteriorates the initially achieved acoustic field focusing. In particular, surface wind-generated waves in winter periods, when the speed of sound in the water layer depends only slightly on the depth (see Fig. 1), prevent one from getting a stable focusing at a distance of 10 km, even for the mild wind velocity, $V \approx 12$ m s^{-1} (Fig. 6). In summer, however, a warm upper layer forms over the shelf, which leads to the build-up of a near-bottom sound channel. The bottom-trapped waveguide modes that propagate in such a channel interact only weakly with the sea surface. As follows from numerical modeling, a stable focusing of sound is possible under these circumstances at a distance of several dozen kilometers for the same wind velocity $V \approx 12$ m s^{-1}. To this end, one needs to single out separate waveguide modes with the assistance of vertical

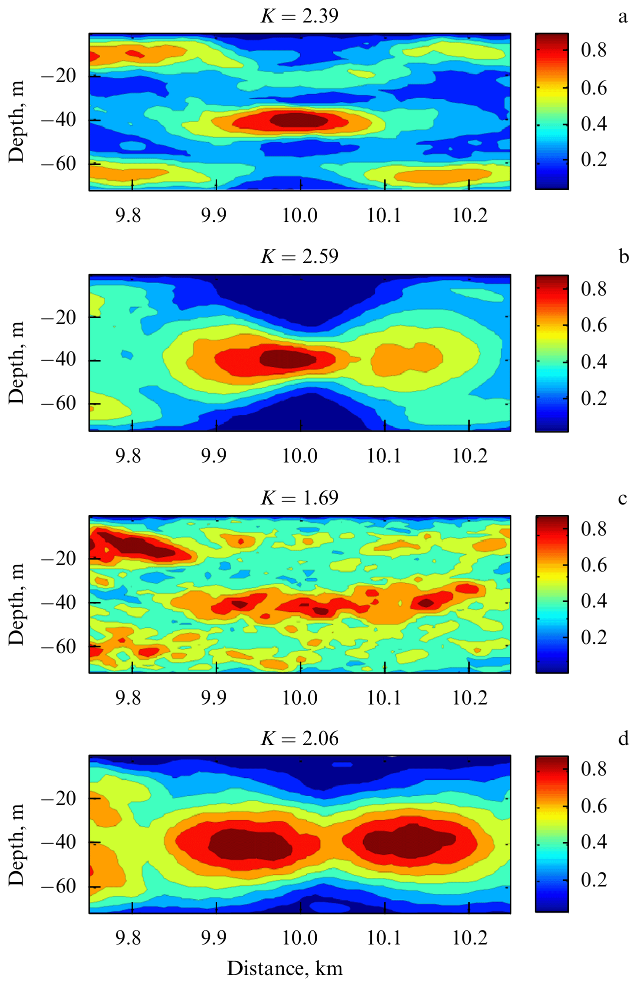

Figure 6. Focusing of sound based on the TRM in the presence of surface waves (numerical simulations): (a) $V = 9$ m s^{-1}, single transceiver at the depth of 9 m; (b) $V = 9$ m s^{-1}, focusing vertical antenna; (c) $V = 12$ m s^{-1}, single transceiver at the depth of 9 m, and (d) $V = 12$ m s^{-1}, focusing vertical antenna.

antennae and use further the sound field with a required mode composition for focusing.

Background internal waves (IWs), observed as a rule in summer, also substantially deteriorate the quality of focusing with time. This deterioration is especially noticeable in open regions of the oceanic shelf (for example, on the U.S. Atlantic Shelf or the Pacific Shelf in the vicinity of Kamchatka), where the intensity of IWs is fairly large. Numerical simulations performed with account for spatio–temporal spectra of the IWs observed in these regions have shown that already at the distance of 20 km the focal spot spreads out and ‘leaves’ the location of the PS under the action of internal waves. Such modifications in the focal spot happen as the IW field correlation time elapses, which takes several hours.

4. Conclusions

In summary, the focused acoustic field in ocean shelf waters exhibits a set of rather unusual physical properties which lay the basis for its wide practical implementation. We list briefly the areas where the focused sound can be applied:

• large-scale acoustical monitoring of the ocean shelf based on measurements of frequency shifts of the sound field interference maxima (including those formed because of focusing) in the frequency domain [8];

• far acoustic underwater communications, for which the focusing not only provides an advantageous signal/noise ratio at the reception point, but also ensures effective suppression of multipath reception [9];

• the acoustic tomography of shallow water, in which case the long-range reverberation can be suppressed owing to focusing [10, 11].

The authors' research results presented in this report were obtained with support from the RFBR (projects 08-02-00283, 10-02-01019, and 11-02-00779).

References

1. Dargeiko M M et al. *Izv. Vyssh. Uchebn. Zaved. Radiofiz.* **27** 746 (1984) [*Radiophys. Quantum Electron.* **27** 516 (1984)]
2. Fink M et al. *Rep. Prog. Phys.* **63** 1933 (2000)
3. Zverev V A *Izbrannye Trudy* (Selected Works) (N. Novgorod: IPF RAN, 2004)
4. Kuperman W et al. *J. Acoust. Soc. Am.* **103** 25 (1998)
5. Zverev V A, Korotin P I, Stromkov A A *Akust. Zh.* **54** 69 (2008) [*Acoust. Phys.* **54** 58 (2008)]
6. Lunkov A A, Petnikov V G, Stromkov A A *Akust. Zh.* **56** 256 (2010) [*Acoust. Phys.* **56** 228 (2010)]
7. Kuz'kin V M et al. *Akust. Zh.* **52** 74 (2006) [*Acoust. Phys.* **52** 65 (2006)]
8. Kuz'kin V M, Pereselkov S A *Akust. Zh.* **53** 833 (2007) [*Acoust. Phys.* **53** 736 (2007)]
9. Edelmann G F et al. *IEEE J. Ocean. Eng.* **27** 602 (2002)
10. Kim S et al. *J. Acoust. Soc. Am.* **115** 1525 (2004)
11. Pereselkov S A, Petnikov V G *Akust. Zh.* **53** 400 (2007) [*Acoust. Phys.* **53** 348 (2007)]

PACS numbers: **43.20.+g**, **43.30.+m**, 43.60.Pt
DOI: 10.3367/UFNe.0181.201111l.1222

Low-mode acoustics of shallow water waveguides

A G Luchinin, A I Khil'ko

1. Introduction

The industrial exploitation of gas and oil fields on the Arctic Shelf and in shallow marginal seas motivates creating information provision with hydroacoustic (HA) facilities aimed, among others, at the tasks of hydroacoustic communications and subsea surveillance. These tasks are usual for underwater acoustics, yet for a long time they were dealt with mainly at moderate distances (1–10 km), when utilizing high-frequency sound waves was efficient [1].

A new stage in the development of underwater acoustics was brought about by using low-frequency (LF) sound to ensure the solution of information tasks over large distances (10^3 km or more) in the deep sea. The research related to such HA systems was initiated abroad by W Munk and colleagues [2] in the 1970s. By the end of the 1970s, Soviet scientists, led by A V Gaponov-Grekhov, actively joined this research. During a short stretch of time they have contributed to the basic principles of LF underwater acoustics, created original low-frequency hydroacoustic (LFHA) transmitters, and carried out experiments in which diffracted LFHA signals have been measured in deep underwater HA channels over long observation distances on record [3].

By the end of 1980, prompted by the increasing interest in the industrial exploitation of the ocean shelf, the realization of HA-observations in extended regions of shallow seas became a pressing issue. In this case, the interaction of an HA field with the sea surface and bottom becomes essential, and, as a result, the field is strongly damped and loses coherence [4]. Moreover, the sound wave propagation is accompanied by high levels of reverberation noise [5]. These effects are the strongest for the interfering multimodal part of LFHA pulses which, as indicated by observations, is unstable in time and rapidly decays. Because of this, past endeavors relying on the usage of individual monopole sources for long-range LF sonar in shallow seas, the increase in their power, or the usage of large receiving arrays failed in providing the necessary progress to solve this problem.

2. The mode shadow and tomographic reconstruction of inhomogeneities

The idea of how to create information HA provision emerged in discussions among A V Gaponov-Grekhov, V I Talanov, V A Zverev, and V V Kovalenko in 1995–1996. Its essence reduces to utilizing only well-propagating LF waveguide (200–400 Hz) modes (in most cases they are also the lower-order modes) for acoustic background illumination of water depth in shallow seas and performing their selective detection. This approach was known in optics and radiophysics but has not been utilized in ocean acoustics.

As confirmed by estimates, such a low-mode-number field, owing to its relatively weak dissipation, should have a larger intensity than a multimode one, given the same energy delivered to the transmitting complex. Additionally, making use of low-mode HA fields could be advantageous in reducing reverberation as a whole and, in particular, the correlation noise from the direct illumination signal if one receives signals belonging to modes of other numbers (it is the shadow principle, also adapted from optics, but in this case applied to modes).

Subsequent analysis has shown that by using the complexly modulated mode pulses, matched to the waveguide, in HA observations in shallow seas it is possible not only to maintain long-distance underwater communications, but also to realize HA sonar through ultimate observation distances. In order to better resolve the underwater landscape over extended sea regions, the method of multistatic (tomographic) surveillance has been adopted, according to which the resultant object image is formed by accumulating projections.

Taking into account all the above-mentioned principles which define the concept of low-mode shallow-sea acoustics, the low-mode pulse acoustic tomography (LMPAT) method has been proposed. Its essence can be formulated as follows. With the help of a set of extended vertical arrays S_i ($i = 1, \ldots, I$), pulse signals corresponding to a particular mode number n are generated, with a sufficiently narrow uncertainty function in the 'frequency–time' parameter plane. The waveguide vertical profile and mode structure are assumed to be known.

Understandably, the excitation of an individual mode is impossible in practice because of the finiteness of the

A G Luchinin, A I Khil'ko Institute of Applied Physics, Russian Academy of Sciences, Nizhny Novgorod, Russian Federation
E-mails: Luch@hydro.appl.sci-nnov.ru, A.khil@hydro.appl.sci-nnov.ru

Uspekhi Fizicheskikh Nauk **181** (11) 1222–1228 (2011)
DOI: 10.3367/UFNr.0181.201111l.1222
Translated by S D Danilov; edited by A Radzig